Organic LETTERS

Letter

pubs.acs.org/OrgLett

β-Amyrin Biosynthesis: The Critical Role of Steric Volume at C-19 of 2,3-Oxidosqualene for Its Correct Folding To Generate the Pentacyclic Scaffold

Tsutomu Hoshino,* Yuki Yamaguchi, Kazunari Takahashi, and Ryousuke Ito

Graduate School of Science and Technology, and Department of Applied Biological Chemistry, Faculty of Agriculture, Niigata University, Ikarashi 2-8050, Nishi-ku, Niigata 950-2181, Japan

Supporting Information

ABSTRACT: The effect of the steric volume at C-19 of (3*S*)-2,3-oxidosqualene **1** on the polycyclization reaction by β-amyrin synthase was examined. The substrate analogs, in which the methyl group at C-19 of **1** was substituted by an ethyl group and hydrogen atom, were converted into the following three new compounds: (17β-H, 20*S*)-20-ethyl-dammara-12,24-diene **9**, β-amyrin homologue **10**, and the 6,6,6,6-fused tetracycle **11**. The folding conformations leading to these products are discussed.

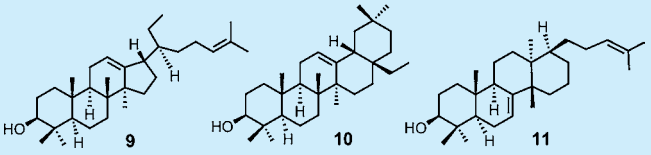

The structural diversity of cyclic triterpenes is remarkable; more than 100 different scaffolds have been isolated to date.[1] The cyclic cores are produced by an enzymatic reaction employing squalene or (3*S*)-2,3-oxidosqualene **1** as a common substrate. The structural diversity of triterpenoids is generated based on the different folding conformation (*chair* or *boat* structure) of the acyclic substrates, Wagner−Meerwein rearrangements of the hydride or methyl group, and deprotonation or hydration of intermediary carbocations generated during the polycyclization cascade.[2] Lanosterol and cycloartenol are produced by folding **1** in a chair−boat−chair−chair conformation to afford the protosteryl cation, followed by 1,2-hydride and methyl shifts. Many genomic sequences encoding triterpene cyclases are currently available. Functional analyses of the active site residues for lanosterol synthase and squalene-hopene cyclase (SHC) have been documented in detail by the Wu group[3] and our group,[4] respectively. In addition to the mutagenesis experiments, the enzymatic cyclization products of substrate analogs have provided deep insight into how the polycyclization reaction is affected by specific modifications, e.g., alteration of the folding conformation leading to different stereochemistry, a truncation of the ring-forming cascade, and a different cation-quenching mode. A number of investigations regarding the enzymatic reactions of substrate analogs with lanosterol synthase[5] and SHC[6] have been reported. However, studies on the mutagenesis[7] and substrate analog[8] of β-amyrin synthase are very limited. It is now accepted that substrate **1** is folded in a chair−chair−chair−boat−boat conformation by β-amyrin synthase (Scheme 1).[9] Protonation of the epoxide triggers the polycyclization cascade to afford a 6,6,6,5-fused tetracyclic dammarenyl cation **3**, which undergoes ring expansion to yield baccharenyl cation **4**. Further cyclization affords a 6,6,6,6,5-fused pentacyclic lupanyl cation **5**, which is then subjected to further ring expansion to yield a 6,6,6,6,6-fused pentacyclic oleanyl cation **6**. Finally, two 1,2-hydride shifts in an antiperiplanar fashion and subsequent H-12 elimination afford β-amyrin **2** as the end product.

Scheme 1. Cyclization Pathway of (3*S*)-Oxidosqualene 1 to β-Amyrin 2

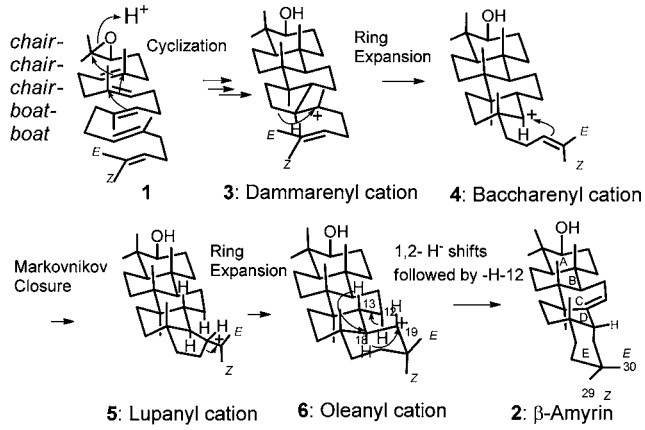

Herein, we report the effect of steric bulk at C-19 of **1** on the polycyclization cascade by employing the recombinant β-amyrin synthase.[7b] The Et-substituted analog **7**[5a] afforded a novel triterpene **9** and β-amyrin homologue **10** (3:1 ratio). 29-Noroxidosqualene **8**[5a] yielded a novel compound **11** consisting of a 6,6,6,6-fused tetracyclic skeleton, as the sole product from the incubation mixture. Figure 1 shows the chemical structures of **1**, **2**, and **7**−**11**. We discuss the cyclization mechanisms for the formation of **9**−**11** and highlight the importance of steric volume at C-19 for the correct folding of **1** to afford **2**.

GC traces of the hexane extracts from the incubation mixtures of **1**, **7**, and **8** with β-amyrin synthase from *Euphorbia*

Received: May 23, 2014
Published: June 24, 2014

   dx.doi.org/10.1021/ol501498q | *Org. Lett.* 2014, 16, 3548−3551

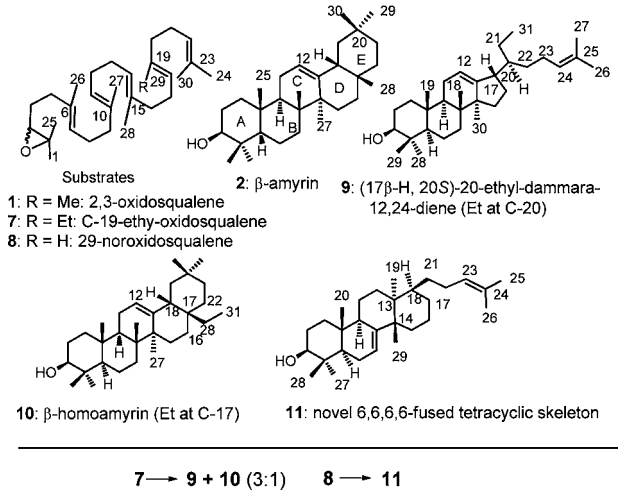

Figure 1. Chemical structures of substrate analogs and products.

tirucalii[7b−d] are depicted in the Supporting Information (SI, Figure S1). Two new products **9** and **10** were produced from **7**, and one product **11** was generated from **8**. As seen from the GC peak areas, the conversion yields of **7** and **8** were less than that of **1** (see also SI, Figure S6A). A large-scale incubation of **7** (23 mg) and repeated incubation of unreacted **7**, which was recovered from the incubation mixture by column chromatography (SiO_2, hexane/EtOAc, 100:0−100:5), were conducted. The cyclic triterpene fraction was acetylated with Ac_2O/Py and the acetates were separated by HPLC (hexane/THF, 100:0.1), resulting in the isolation of the pure acetates of **9** (5.9 mg) and **10** (1.5 mg).

^1H and ^{13}C NMR analyses of **9**-Ac suggested the presence of two double bonds (600 MHz, C_6D_6, δ_H 5.42, bs, 1H, H-12; 5.46, t, J = 6.8 Hz, 1H, H-24; δ_C 118.1, d, C-12; 146.0, s, C-13; 125.7, d, C-24; 130.8, s, C-25). The two olefinic methyl protons (δ_H 1.85, s, 3H; 1.78, s, 3H) had definitive HMBC cross peaks with C-24 and C-25, indicating that the terminal isopropylidene moiety remained unreacted. This finding indicated that **9**-Ac was composed of a tetracyclic ring system. Me-30 (δ_H 1.15, s, 3H) had a strong HMBC correlation with C-13, indicating that the second double bond was situated at C-12 and C-13. Strong NOEs between H-3, H-5, H-9, and Me-30 showed an α-configuration for Me-30. Unambiguous NOEs between Me-19 (δ_H 0.865, s, 3H), Me-18 (δ_H 1.06, s, 3H), and H-17 (δ_H 2.28, m, 1H) revealed the β-configuration of H-17. Thus, product **9** was assigned as tetracyclic 20-ethyl-dammara-12,24-dien-3β-ol with 17β-H (SI, Figure S2). The stereochemistry at C-20 is yet to be determined. Energy-minimized conformations of 20*R*- and 20*S*-compounds were simulated using Chem3D and MM2 programs (SI, Figure S3). The NOE between H-17 and H-20 is anticipated for 20*R*-**9**, but no corresponding NOE is expected for 20*S*-**9**. This method has been applied to determine the stereochemistry at C-20 of isohelianol[10a] and (17β-H, 20*R*)-dammara-12,24-dien-3β-ol (isolated from *Clusia guaviarensis*).[10b] Indeed, no NOE was observed for product **9** (SI, Figures S2−7 and Figure S3), thus supporting that **9** has a 20*S*-configuration. In the ^1H NMR spectrum of **7**, the vinylic Me protons appeared at δ_H 1.5−1.8 ppm; however, all Me protons of **10**-Ac resonated at higher field, indicating that **10** was a fully cyclized product. One double bond was found (δ_H 5.36, t, J = 3.4 Hz, H-12; δ_C 122.4, d, C-12; 145.1, s, C-13). The HMBC cross peak was observed between Me-27 (δ_H 1.36, s, 3H) and C-13, proving that the double bond of **10** was positioned at C-12 and C-13. Strong NOEs between H-3, H-5, H-9, and Me-27 demonstrated that all the protons had α-configuration. α-Oriented Me-27 also had no NOE cross peak with H-28 (δ_H 1.16, m; 1.83, m). A definitive NOE was observed between H-28 and H-18, indicating that they had a β-configuration. A strong NOE between H-28 and Me-30 enabled the assignment of Me-30 (δ_H 1.07, s, 3H). Therefore, detailed 2D NMR analyses (SI, Figure S4) indicated that **10** was the β-amyrin homologue with an ethyl group at C-17.

Incubation of (±)-analog **8** (24 mg) with β-amyrin synthase showed significantly low conversion yield (SI, Figure S1). To obtain sufficient amounts of **11** or structural determination, unreacted **8** was recovered and subjected to repeated incubations. The cyclic triterpene-rich fraction was acetylated with Ac_2O/Py, followed by HPLC (hexane/THF, 100:0.005), to afford pure **11**-Ac (1.4 mg). The ^1H NMR spectrum (400 MHz, C_6D_6) showed two olefinic protons (δ_H 5.45, bs, 1H, H-7; 5.42, t, J = 6.8 Hz, 1H, H-23). The characteristic peaks of the terminal isopropylidene moiety from **1** still remained in **11**-Ac. The two Me groups (δ_H 1.85, s, 3H, Me-25; δ_H 1.74, s, 3H, Me-26) had clear HMBC cross peaks for C-23 (δ_C 125.5, d) and C-24 (δ_C 131.1, s), suggesting that **11**-Ac was a tetracyclic molecule. The $^1H-^1H$ COSY and HOHAHA spectra definitively verified the proton correlations of H-23 to H-18 (δ_H 1.32, m, 1H) and those of H-18 to H-15 (SI, Figures S5−10, S5−19). The protons of H-22, H-21, H-17, H-16, and H-15 were inferred to be methylene protons from the DEPTs and HSQC data. In the HMBC spectrum, both Me-29 (δ_H 1.16, s, 3H) and Me-19 (δ_H 1.29, s, 3H) had clear correlations with C-13 (δ_C 37.55, s) and C-14 (δ_C 40.51, s), while Me-29 and Me-19 had a cross peak with C-15 (δ_C 33.90, t) and C-18 (δ_C 46.10, d), respectively. Thus, a 6-membered skeleton was assigned for the D-ring. An HMBC correlation between Me-29 and C-8 (δ_C 147.4, s) and the chemical shift of H-9 (δ_H 2.25, bd, J = 13 Hz, 1H) clearly indicated that the double bond was situated at C-7 and C-8. The strong NOEs between Me-29 and H-21, Me-19 and H-9, and H-5 and H-9 verified the α-orientation of Me-19 and β-disposition of the side chain at C-18. Therefore, detailed NMR analyses (SI, Figure S5) indicated the structure of **11** as depicted in Figure 1.

Scheme 2A depicts the polycyclization pathway of **7** for the formation of **9** and **10**. The proton, released from the DCTA motif,[7b] protonated the epoxide of the folded chair−chair−chair−chair conformation **12** and afforded the 6,6,5-fused tricyclic Markovnikov cation **13**. Subsequent ring expansion yielded a 6,6,6-fused tricycle **14**. Further cyclization afforded the 6,6,6,5-fused tetracycle **15**. 1,2-Hydride shifts (H-17β → C-20; H-13β → C-17), followed by deprotonation of H-12α, afforded 20-ethyl-dammara-12,24-diene **9** with 20*S*-stereochemistry. The Et-substituent at C-19 of **7** was arranged in an α-configuration during the cyclization reaction, which differs from the β-arrangement in **1**. In addition to the misfolding conformation shown in **12**, Et analog **7** partially underwent a normal polycyclization cascade, affording β-amyrin homologue **10** via path *a* shown in Scheme 2B (see also Scheme 1). Because of a larger steric volume, a lesser amount of the Et moiety was accommodated inside the β-arranged cleft of the cyclase compared to the Me-29 residue of **1**. Consequently, steric repulsion enforced the α-orientation of the Et group (Scheme 2, marked with shaded closed curve), affording chair folding conformation for the D-ring formation. The minimal motion of the side chain led to the 20*S*-configuration, as shown

dx.doi.org/10.1021/ol501498q | *Org. Lett.* 2014, 16, 3548−3551

Scheme 2. Cyclization Pathways of 7 into 9 and 10 (A and B), and 8 into 11 (C)

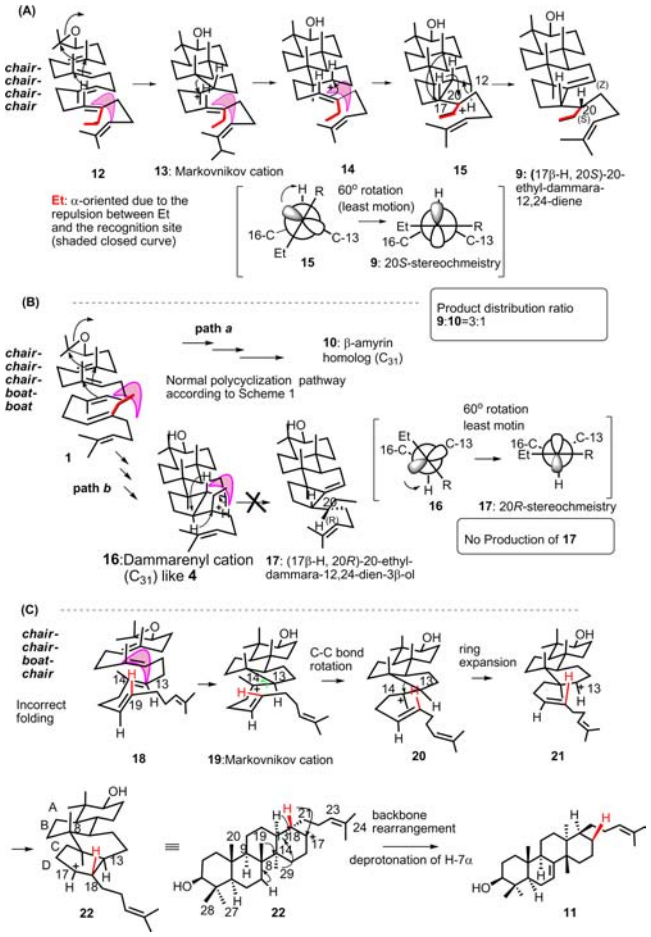

in the Newman projection of **15** (Scheme 2A).[5e,11] The 20*R*-configuration is less favored because of the requirement of greater rotational movement such as 120° in the reaction cavity.[5e,11] On the other hand, it is surmised that a chair−chair−chair−boat−boat conformation **1** (normal folding conformation; see path *b* in Scheme 2B) would afford 20*R*-stereochemistry because of the least amount of motion of the side chain; however, **17** was not found in the incubation mixture. Production of **10** indicated that the slightly large steric volume of the Et group at C-19 could be tolerated at the cleft responsible for binding Me-29.

Scheme 2C shows the proposed biosynthetic pathway to afford the novel carbocyclic skeleton **11**. Substrate **8** was folded in a chair−chair−boat−chair conformation **18**. Protonation[7b] of the epoxide afforded Markovnikov cation **19** composed of a 6,6,5-fused tricycle. Bond rotation about the C-13 to C-14 axis afforded **20**. This rotational process is required to fulfill the stereochemistry of end-product **11**. Intermediate **20** underwent a ring expansion to yield 6,6,6-fused tricycle **21**. Further cyclization reaction afforded 6,6,6,6-fused tetracyclic core **22**. Sequential 1,2-hydride and Me group shifts (backbone rearrangement) occurred in an antiperiplanar fashion (H-18β → C-17β, H-13α → C-18α, Me-29α → C-13α, Me-19β → C-14β), followed by elimination of H-7α, to afford **11**. Notably, the conformations of the C- and D-rings were changed from chair to boat and from boat to chair form, respectively. We were keen to investigate why the unusual chair−chair−boat−chair conformation of **8** was constructed during the polycyclization cascade. As described above, the binding site of Me-29 is somewhat loosely packed, affording β-homoamyrin **10** under the control of normal folding. In turn, the interaction between the less bulky hydrogen atom at C-19 and the loosely packed binding site may lead to more space and mobility at the D-ring-formation site, forming the thermodynamically favored chair conformation instead of the constrained boat form. Furthermore, the improper arrangement of **8** in the binding site could further contribute to the misfolded boat form at the C-ring-formation site. The increased space at the D-ring-formation site could further allow the C-13 to C-14 bond rotation in **19** prior to ring expansion; a rotation would be unlikely if the substrate had been tightly constrained in the enzyme active site. We were intrigued by the formation of a 6-membered rather than 5-membered D-ring for **11**. Upon ring formation, intermediate cation **21** affords only a secondary cation irrespective of the formation of 5- or 6-membered D-rings, unlike intermediate **3** that affords a more stable tertiary carbocation during the formation of a 5-membered ring (Scheme 1). Therefore, the 6-membered is favored over the 5-membered D-ring for **11** because of its lesser steric strain. The misfolded conformation for the C/D-ring formation prohibited further annulation reaction, halting the polycyclization cascade at the premature tetracyclic stage.

To evaluate the β-amyrin synthase substrate preference, the conversion yields of **1**, **7**, and **8** were estimated (SI, Figure S6A). Et-substituted analog **7** had a relatively high conversion yield (*ca.* 70%), while **8** had a significantly decreased yield (*ca* 3%), suggesting that this cyclase may have undergone a strong time-dependent inhibition by **8**.[12] After preincubation of **8** with this enzyme at 30 °C for specific time intervals (0, 0.5, 1, 2, 4, 6 h), **1** was added and incubation was continued for 1 h. Afterward, the amounts of β-amyrin **2** produced were estimated. Longer preincubation times reduced the production of **2**, indicating a time-dependent inactivation by **8**. Increased addition of **8** caused stronger inhibition (SI, Figure S6B). The k_{inact}, K_i, and IC_{50} values were determined to be 9.6 h^{-1}, 124 μM, and 14.7 μM, respectively (SI, Figure S6C, D). This inactivation would have been caused by covalent bond formation of this cyclase with intermediary cations **19**−**22**. In contrast, the cyclization yield of analog **7** was much higher and can be ascribed principally to a looser binding of **7** with this cyclase, because a bulkier Et group was incorporated on **1**.

SHC catalyzes the formation of the 6,6,6,6,5-fused pentacyclic hopene **23** and hopanol **24** (SI, Figure S7) by folding the squalene substrate in an all-chair conformation.[2a] Previously, we reported that 28-norhopanoid scaffolds (**25**, **26**, Figure S7) were produced by incubating 29-norsqaulene with SHC, demonstrating that the decreased size at C-19 has little effect on the folding conformation.[6f] On the other hand, the decreased steric size at C-19 exerts a significant effect on the polycyclization pathway for the biosyntheses of lanosterol (**28**, **29**, Figure S7)[5a] and β-amyrin (**11**). When the bulkier Et-analog **7** was employed as the substrate, lanosterol synthase gave homolanosterol (**27**, Et at C-20) as a sole product,[5a] while β-amyrin synthase afforded both **9** and **10**. A higher ratio of production of tetracycle **9** to that of pentacycle **10** (3:1) indicated that the cleft of β-amyrin synthase that accepts Me-29 of **1** is more compact than that of lanosterol synthase. This compactness, but somewhat loosely packed to tolerate the Et-substituent, allowed the terminal isoprene moiety to access tetracyclic cation **3**, which undergoes ring expansion to form

dx.doi.org/10.1021/ol501498q | *Org. Lett.* 2014, 16, 3548−3551

cation **4**, leading to further cyclization to construct the E-ring. However, no further cyclization is needed for the biosynthesis of tetracyclic lanosterol.

In conclusion, we have created novel triterpene scaffolds **9**, **10**, and **11** by employing analogs **7** and **8**. In nature, a 6,6,6,6-fused tetracyclic triterpene scaffold (C_{30}) equivalent to that of nortriterpene **11**, which differs from baccharenyl skeleton **4**, is yet to be found (SI, Figure S8). This can be ascribed to the structural feature of **1**, in which a Me group is substituted at C-19, leading to the formation of a 5-membered D-ring (tertiary cation **3**) under Markovnikov control. The steric volume at C-19 plays a key role in the correct folding of **1** into a chair−chair−chair−boat−boat conformation to generate **2**. Furthermore, the effect of the steric bulk difference at C-19 on the polycyclization pathways depends on the class of triterpene cyclase.

■ ASSOCIATED CONTENT

Supporting Information

Spectroscopic data including EIMS and NMR, and additional experimental data (GC and enzyme kinetics). This material is available free of charge via the Internet at http://pubs.acs.org.

■ AUTHOR INFORMATION

Corresponding Author

*E-mail: hoshitsu@agr.niigata-u.ac.jp.

Notes

The authors declare no competing financial interest.

■ ACKNOWLEDGMENTS

This work was supported in part by Grant-in-Aid for Scientific Research from the Japan Society for the Promotion of Science (Nos. 25450150 and 18380001).

■ REFERENCES

(1) Xu, R.; Fazio, G. C.; Matsuda, S. P. T. *Phytochemistry* **2004**, *65*, 261−291.

(2) Reviews: (a) Hoshino, T.; Sato, T. *Chem. Commun.* **2002**, 291−301. (b) Wend, K. U.; Schulz, G. E.; Corey, E. J.; Liu, D. R. *Angew. Chem., Int. Ed.* **2000**, *39*, 2812−2833. (c) Yoder, R. A.; Johnston, J. N. *Chem. Rev.* **2005**, *105*, 4730−4756. (d) Wu, T. K.; Chang, C. H.; Liu, Y. T.; Wang, T. T. *Chem. Rec.* **2008**, *8*, 302−305. (e) Abe, I. *Nat. Prod. Rep.* **2007**, *24*, 1311−1331. (f) Nes, W. D. *Chem. Rev.* **2011**, *111*, 6423−6451.

(3) (a) Chang, C. H.; Wen, H. Y.; Shie, W. S.; Liu, C. T.; Li, M. E.; Liu, Y. T.; Li, W. H.; Wu, T. K. *Org. Biomol. Chem.* **2013**, *11*, 4214−4219. (b) Chang, C. H.; Chen, Y. C.; Tseng, S. W.; Liu, Y. T.; Wen, H. Y.; Li, W. H.; Huang, C. Y.; Ko, C. Y.; Wang, T. T.; Wu, T. K. *Biochimie* **2012**, *94*, 2376−2381. (c) Wu, T. K.; Chang, C. H.; Wen, H. Y.; Liu, Y. T.; Li, W. H.; Wang, T. T.; Shie, W. S. *Org. Lett.* **2010**, *12*, 500−503.

(4) (a) Morikubo, N.; Fukuda, Y.; Ohtake, K.; Shinya, N.; Kiga, D.; Sakamoto, K.; Asanuma, M.; Hirota, H.; Yokoyama, S.; Hoshino, T. *J. Am. Chem. Soc.* **2006**, *128*, 13184−13194. (b) Hoshino, T.; Shimizu, K.; Sato, T. *Angew. Chem., Int. Ed.* **2004**, *43*, 6700−6703. (c) Sato, T.; Hoshino, T. *Biosci. Biotechnol. Biochem.* **2001**, *65*, 2233−2242. (d) Hoshino, T.; Abe, T.; Kouda, M. *Chem. Commun.* **2000**, 441−442.

(5) (a) Hoshino, T.; Chiba, A.; Abe, N. *Chem.—Eur. J.* **2012**, *18*, 13108−13116. (b) Hoshino, T.; Sakai, Y. *Tetrahedron Lett.* **2001**, *42*, 7319−7323. (c) Hoshino, T.; Sakai, Y. *Chem. Commun.* **1998**, 1591−1592. (d) Hoshino, T.; Ishibashi, E.; Kaneko, K. *J. Chem. Soc., Chem. Commun.* **1995**, 2401−2402. (e) Corey, E. J.; Virgil, S. C. *J. Am. Chem. Soc.* **1991**, *113*, 4025−4026. (f) Corey, E. J.; Virgil, S. C.; Sarshar, S. *J. Am. Chem. Soc.* **1991**, *113*, 8171−8172. (g) van Tamelen, E. E.; Hanzlik, R. P.; Sharpless, K. B.; Clayton, R. B.; Richter, W. J.; Burlingame, A. L. *J. Am. Chem. Soc.* **1968**, *90*, 3284−3286.

(6) (a) Yonemura, Y.; Ohyama, T.; Hoshino, T. *Org. Biomol. Chem.* **2012**, *10*, 440−446. (b) Hoshino, T.; Kumai, Y.; Sato, T. *Chem.—Eur. J.* **2009**, *15*, 2091−2100. (c) Abe, T.; Hoshino, T. *Org. Biomol. Chem.* **2005**, *3*, 3127−3139. (d) Hoshino, T.; Nakano, S.; Kondo, T.; Sato, T.; Miyoshi, A. *Org. Biomol. Chem.* **2004**, *2*, 1456−1470. (e) Hoshino, T.; Kumai, Y.; Kudo, I.; Nakano, S.; Ohashi, S. *Org. Biomol. Chem.* **2004**, *2*, 2650−2657. (f) Nakano, S.; Ohashi, S.; Hoshino, T. *Org. Biomol. Chem.* **2004**, *2*, 2012−2022. (g) Hoshino, T.; Ohashi, S. *Org. Lett.* **2002**, *4*, 2553−2556.

(7) (a) Kushiro, T.; Shibuya, M.; Masuda, K.; Ebizuka, Y. *J. Am. Chem. Soc.* **2000**, *122*, 6816−6824. (b) Ito, R.; Masukawa, Y.; Hoshino, T. *FEBS J.* **2013**, *280*, 1267−1280. (c) Ito, R.; Hashimoto, I.; Masukawa, Y.; Hoshino, T. *Chem.—Eur. J.* **2013**, *19*, 17150−17158. (d) Ito, R.; Masukawa, Y.; Nakada, C.; Amari, K.; Nakano, C.; Hoshino, T. *Org. Biomol. Chem.* **2014**, *12*, 3836−3846.

(8) (a) Corey, E. J.; Gross, S. K. *J. Am. Chem. Soc.* **1968**, *90*, 5045−5046. (b) Abe, I.; Sakano, Y.; Tanaka, H.; Lou, W.; Noguchi, H.; Shibuya, M.; Ebizuka, Y. *J. Am. Chem. Soc.* **2004**, *126*, 3426−3427. (c) Abe, I.; Sakano, Y.; Sodeyama, M.; Tanaka, H.; Noguchi, H.; Shibuya, M.; Ebizuka, Y. *J. Am. Chem. Soc.* **2004**, *126*, 6880−6881.

(9) (a) Eschenmoser, A.; Ruzicka, L.; Jeger, O.; Arigoni, D. *Helv. Chim. Acta* **1955**, *38*, 1890−1940. (b) Suga, T.; Shishibori, T. *Phytochemistry* **1975**, *14*, 2411−2417.

(10) (a) Akihisa, T.; Kimura, Y.; Koike, K.; Shibata, T.; Yoshida, Z.; Nikaido, T.; Tamura, T. *J. Nat. Prod.* **1998**, *61*, 409−412. (b) Akihisa, T.; Olivares, E. M.; Kimura, Y.; Ukiya, M.; Monache, F. D. *J. Jpn. Oil Chem. Soc.* **1999**, *48*, 1303−1306.

(11) Abe, I.; Rohmer, M. *J. Chem. Soc., Perkin Trans. 1* **1994**, 783−791.

(12) Lim, H.-K.; Duczak, N., Jr.; Brougham, L.; Elliot, M.; Patel, K.; Chan, K. *Drug Metab. Dispos.* **2005**, *33*, 1211−1219.